IEEE Access
Multidisciplinary | Rapid Review | Open Access Journal

Received October 21, 2021, accepted December 3, 2021, date of publication December 14, 2021,
date of current version December 28, 2021.

Digital Object Identifier 10.1109/ACCESS.2021.3135496

MATPOWER-Based Harmonic Power Flow Analysis for Power Systems With Passive Power Filters

NIEN-CHE YANG, (Member, IEEE), AND EUNIKE WIDYA ADINDA
Department of Electrical Engineering, National Taiwan University of Science and Technology, Taipei 10607, Taiwan

Corresponding author: Nien-Che Yang (ncyang@mail.ntust.edu.tw)

This work was supported in part by the Ministry of Science and Technology (MOST), Taiwan, under Grant MOST 109-3111-8-011-001; and in part by the DELTA-National Taiwan University of Science of Technology (NTUST) Joint Research Center.

ABSTRACT As an open-source MATLAB-based power system simulation package, Matpower has been proven to have an adjustable feature that supports modifications to solve specific problems in power systems. Since it was first released, the Matpower framework has been widely used for solving steady-state electric power scheduling problems. However, a modification to solve a harmonic power flow (HPF) using Matpower has not been launched yet. This paper presents modification procedures to customize the network component models and problem formulations in Matpower for the HPF study. The modification procedures can be used to evaluate the bus admittance matrix, bus voltages, and current sources for any harmonic order. Moreover, the modified Matpower can evaluate the passive power filter (PPF) installation to improve the harmonic distortion in power systems. The simulation results were satisfactory, indicating that the modification enabled solving problems in both fundamental and harmonic power flows.

INDEX TERMS Bus admittance, bus voltage, harmonic power flow analysis, nonlinear loads, passive power filters.

I. INTRODUCTION

Nonlinear devices have currents disproportional to the applied voltages, resulting in distorted current and voltage waveforms [1]. The resulting harmonic may lead to several power-quality problems that require attention. To resolve this harmonic issue, network component models in power systems must be adequately designed. In some studies, researchers assumed all loads to be linear. However, this assumption is typically unrealistic [2], as most electric loads in power systems are not uniform in terms of power use. Nonlinear loads are widely used. Therefore, to appropriately address load modeling, load models should include linear and nonlinear loads [3]. Simultaneously, nonlinear loads may distort the power systems by injecting harmonic currents. An inaccurate assumption of load modeling may magnify the harmonic voltage and current at undesired resonance harmonic frequencies. In addition, the sizing and sitting of harmonic-source components, referred to as nonlinear loads, should be adequately evaluated to reduce the harmonic distortion in power systems and improve the power quality.

The associate editor coordinating the review of this manuscript and approving it for publication was Snehal Gawande.

To improve the power quality of power systems, shunt capacitors (SCs) are commonly installed as voltage controllers, power-factor correctors, and reactive power compensators [4], [5]. Hypothetically, SCs reduce the reactive current flow through the power system by injecting reactive power and supporting the system voltage during voltage reduction contingencies [6]. However, the installation of SCs in a power system with harmonic loads may produce harmonic resonance, which leads to more harmonic issues [7]. These issues may be overcome by installing power filters (PFs), reducing harmonic distortion [8]. There are three types of PFs: passive PFs (PPFs), active PFs, and hybrid active PFs. PPFs offer a simple design, are more economical than the other types [9], and provide low-impedance shunt paths for harmonic current injection [10]. It is essential to determine the PPF types, locations, sizes, and parameters for harmonic mitigation. Thus, an appropriate harmonic power flow (HPF) study based on Matpower is proposed considering the installation of SCs and PPFs.

Matpower [11] is an open-source simulation package available in MATLAB and provides numerous case examples. For research and education purposes, Matpower is widely used to analyze a power system, addressing steady-state and balanced system problems, from power flow to optimal power

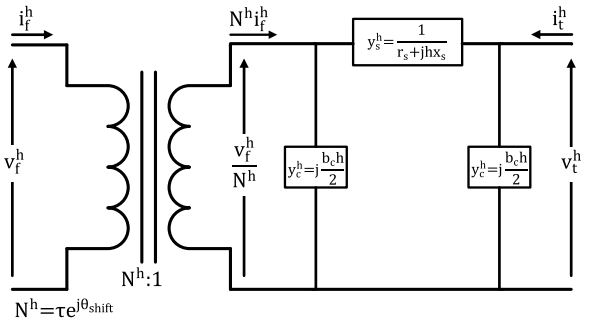

FIGURE 1. Branch model.

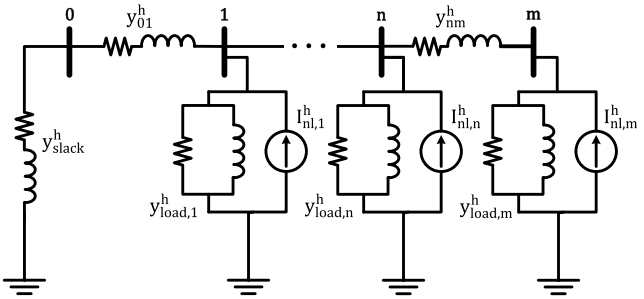

FIGURE 2. Equivalent load model at the h-th harmonic frequency.

flow (OPF) analysis. In Matpower, the Y_{bus} matrix of FPF considers the branches and shunt elements, excluding the loads and PPF models. In this study, a modification procedure is proposed to address the loads and PPF modeling in a Y_{bus} matrix for HPF analysis.

This modified Matpower offers an adjustable feature and a simple running process in a one-shot simulation for performing the HPF analysis. In Sections II and III, the network component models and the proposed modification algorithm are introduced, respectively. The simulation results are presented in Section IV, and conclusions are provided in Section V.

II. MODELING OF NETWORK COMPONENTS

In Matpower, the power system is modeled as a balanced network system. A per-unit system was used for the equation formulations. Consequently, all electrical quantities are expressed per unit. Moreover, the network component models are represented in vector and matrix forms. For the HPF study, additional data were used to modify the fundamental data and network component models used in Matpower [12].

A. CASE DATA FORMATS

For the HPF study, it is mandatory to include additional data matrices in the case M-file. These additional data are described as `nlbus` for nonlinear load sitting and size, `h` for harmonic order, `Ih` for the harmonic spectrum of each harmonic order, and `ppf` for PPF data, including the types, locations, size, and parameters (resistance, inductance, and capacitance) of PPFs. The number of columns in `bus`, `branch`, `h`, and PPF matrices are represented as `nb`, `nl`, `nh`, and `nppf`, respectively.

B. BRANCHES

In this study, an original branch model from Matpower was used and modified, as shown in Fig. 1. The branch model with a standard π-transmission line model, consisting of a series admittance (y_s^h) and total charging capacitance (b_c), was modified for harmonic calculations. The transformer model has a magnitude (τ) and phase-shift angle (θ_{shift}^h). For the HPF study, the phase-shift angle should be incorporated into harmonic penetration [13]. For the h-harmonic order, the N ratio is expressed as:

$$N^h = \tau e^{j\theta_{shift}^h} \tag{1}$$

From Fig. 1, it can be seen that the series admittance of the harmonic component model for the h-th harmonic order is determined by:

$$y_s^h = \frac{1}{r_s + h \cdot jx_s} \tag{2}$$

In addition, the total charging capacitance is determined by:

$$y_c^h = h \cdot \frac{b_c}{2} \tag{3}$$

Therefore, the branch admittance matrix can be written as:

$$Y_{br}^h = \begin{bmatrix} (y_s^h + jy_c^h)\frac{1}{\tau^2} & -y_s^h \frac{1}{\tau e^{-j\theta_{shift}^h}} \\ -y_s^h \frac{1}{\tau e^{j\theta_{shift}^h}} & y_s^h + jy_c^h \end{bmatrix} \tag{4}$$

Furthermore, the branch admittance matrix can be simplified by labeling each element as:

$$Y_{br,ij}^h = \begin{bmatrix} y_{ff,ij}^h & y_{ft,ij}^h \\ y_{tf,ij}^h & y_{tt,ij}^h \end{bmatrix} \tag{5}$$

for branch ij at the h-th harmonic order.

C. LOADS

The equivalent load model for the HPF analysis is presented in Fig. 2 [3]. Unlike the FPF, nonlinear loads are regarded as harmonic current sources. The combination of the loads (nonlinear and linear loads) is expressed as admittances included in the harmonic admittance matrix Y_{bus}^h.

The linear loads are specified as real ($P_{d,i}$) and reactive ($Q_{d,i}$) power demands at bus-i. The impedance of the linear load at bus-i can be calculated by:

$$r_{d,i} + jx_{d,i} = \frac{|V_{base,i}|^2}{P_{d,i} - jQ_{d,i}} \tag{6}$$

Hence, the linear loads in the admittance form for the h-th harmonic order are expressed as:

$$y_{load,i}^h = \frac{1}{r_{d,i} + h \cdot jx_{d,i}} \tag{7}$$

TABLE 1. Typical harmonic spectrum.

Harmonic Order	Typical Harmonic Spectrum	
	$I^h_{spectrum}(\%)$	$\theta^h_{spectrum}(^\circ)$
1	100	0
5	18.24	-55.68
7	11.90	-84.11
11	5.73	-143.56
13	4.01	-175.58
17	1.93	111.39
19	1.39	68.30
23	0.94	-24.61
25	0.86	-67.64
29	0.71	-145.46
31	0.62	176.83
35	0.44	97.40
37	0.38	54.36

D. HARMONIC CURRENT SOURCES AND SPECTRUM

As a harmonic current source, the fundamental demand currents for nonlinear loads are described as follows:

$$I^{h=1}_{inj,i} = \left(\frac{P_{nl,i} + jQ_{nl,i}}{V_i}\right)^* \tag{8}$$

Considering the harmonic characteristics, the injected currents for each harmonic order can be calculated using (9) and (10) with the typical harmonic spectrum defined in Table 1 for harmonic orders 1–37.

$$I^h_{inj,i} = I^h_{spectrum} \cdot I^{h=1}_{inj,i} \tag{9}$$

$$\theta^h_{inj,i} = h\theta^{h=1}_{inj,i} + \theta^h_{spectrum} \tag{10}$$

In the modified Matpower, the harmonic spectrum in the case format is presented in the I_h matrix in the case M-file for each harmonic order, h, at the specific bus-i.

E. SHUNT CAPACITORS

In the original Matpower, the shunt elements, used to model capacitors or inductors connected to a power system, are represented as G_S and B_S, respectively, and modeled as a fixed admittance to the ground at bus-i described below.

$$Y^{h=1}_{sc,i} = G_{sc,i} + jB_{sc,i} \tag{11}$$

In this study, the ideal SCs injected Mvar into the power system at the rated voltage with zero phase-angle displacements, represented as B_S. Then, the admittance of SCs at bus-i for the h-th harmonic order can be calculated using (13).

$$X_{sc,i} = \frac{V^2_{base,i}}{B_{sc,i}} \tag{12}$$

$$Y^h_{sc,i} = \frac{h}{-jX_{sc,i}} \tag{13}$$

F. PASSIVE POWER FILTERS

The PPFs provide a low-impedance path for critical harmonic currents to eliminate harmonic distortions and are commonly located near nonlinear loads. The admittance of PPFs should be considered in both the FPF and HPF studies.

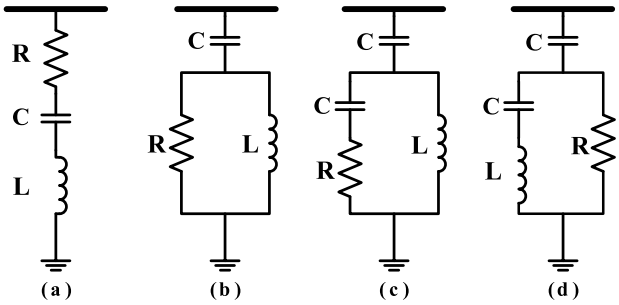

FIGURE 3. Typical PPFs: (a) single-tuned PPF, (b) second-order damped PPF, (c) third-order damped PPF, and (d) C-type damped PPF.

The configurations of the PPF types are shown in Fig. 3, and the impedances at the h-th harmonic order are described in (14) to (17).

(a) Second-order damped PPF

$$Z^h_{PPF,i} = R_i + j\left(hX_{L,i} - \frac{X_{C,i}}{h}\right) \tag{14}$$

(b) Third-order damped PPF

$$Z^h_{PPF,i} = \frac{R_i\left(hX_{L,i}\right)^2}{R_i^2 + \left(hX_{L,i}\right)^2} + j\left[\frac{R_i^2 hX_{L,i}}{R_i^2 + \left(hX_{L,i}\right)^2} - \frac{X_{C,i}}{h}\right] \tag{15}$$

(c) Third-order damped PPF

$$Z^h_{PPF,i} = \frac{R_i\left(hX_{L,i}\right)^2}{R_i^2 + \left(hX_{L,i} - \frac{X_{C,i}}{h}\right)^2} + j\left[\frac{R_i^2 hX_{L,i} - hX^2_{L,i}X_{C,i} + \frac{X_{L,i}X^2_{C,i}}{h}}{R_i^2 + \left(hX_{L,i} - \frac{X_{C,i}}{h}\right)^2} - \frac{X_{C,i}}{h}\right] \tag{16}$$

(d) C-Type PPF

$$Z^h_{PPF,i} = \frac{R_i\left(hX_{L,i} - \frac{X_{L,i}}{h}\right)^2}{R_i^2 + \left(hX_{L,i} - \frac{X_{L,i}}{h}\right)^2} + j\left[\frac{R_i^2\left(hX_{L,i} - \frac{X_{L,i}}{h}\right)}{R_i^2 + \left(hX_{L,i} - \frac{X_{L,i}}{h}\right)^2} - \frac{X_{C,i}}{h}\right] \tag{17}$$

For a single-tuned PPF, the resonant harmonic order is calculated using (18), and R is defined as the internal resistance of the reactor and capacitor, which can be neglected.

$$h_{nh} = \frac{1}{2\pi f\sqrt{LC}} \tag{18}$$

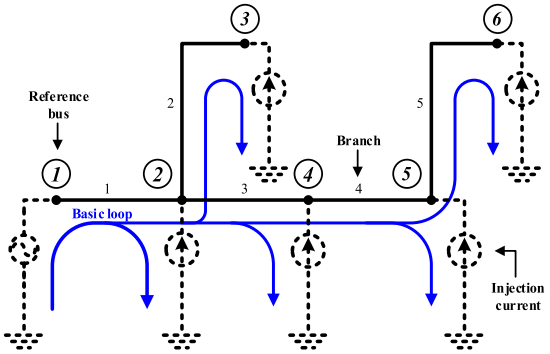

FIGURE 4. One-line diagram of a simple radial distribution system.

For all PPF types, the inductance and capacitance reactances are defined as follows:

$$X_{L,i} = 2\pi fL \tag{19}$$

$$X_{C,i} = \frac{1}{2\pi fC} \tag{20}$$

G. CONNECTION MATRICES

In a network with n_b buses, the connection matrices, C_f and C_t, define the connection between the starting and ending buses in branch-i, which are illustrated as bus-j and bus-k, respectively. These matrices contain "1" values for $(i, j)^{th}$ elements of C_f and C_t, whose size is $n_{branch} \times n_b$ for each matrix with the number of branches of:

$$n_{branch} = n_b - 1 \tag{21}$$

and the connection matrices C_f and C_t are defined by (22) and (23), as shown at the bottom of the next page, respectively. For a simple system in Fig. 4, the connection matrices C_f and C_t are expressed in Equations (24) and (25), as shown at the bottom of the next page.

H. NETWORK PERFORMANCE EQUATION

All the network component models in the admittance form described above are incorporated into $Y_{bus}^{h=1}$ and Y_{bus}^{h} matrices. For the HPF study, the Y_{bus}^{h} matrix denotes a complex $n_b \times n_b$ matrix for each harmonic order.

The fundamental admittance matrix, $Y_{bus}^{h=1}$, considering all the admittance elements becomes:

$$Y_f^{h=1} = \left[Y_{ff}^{h=1}\right][C_f] + \left[Y_{ft}^{h=1}\right][C_t] \tag{26}$$

$$Y_t^{h=1} = \left[Y_{tf}^{h=1}\right][C_f] + \left[Y_{tt}^{h=1}\right][C_t] \tag{27}$$

$$\left[Y_{bus}^{h=1}\right] = \left[C_f^T\right]\left[Y_f^{h=1}\right] + \left[C_t^T\right]\left[Y_t^{h=1}\right] + \left[Y_{sc}^{h=1}\right] + \left[Y_{ppf}^{h=1}\right] \tag{28}$$

Corresponding to the formation of the $Y_{bus}^{h=1}$, the Y_{bus}^{h} matrix with nonlinear loads as the harmonic source and the installation of SCs and PPFs can be formed as follows:

$$Y_f^h = \left[Y_{ff}^h\right][C_f] + \left[Y_{ft}^h\right][C_t] \tag{29}$$

$$Y_t^h = \left[Y_{tf}^h\right][C_f] + \left[Y_{tt}^h\right][C_t] \tag{30}$$

$$\left[Y_{bus}^h\right] = \left[C_f^T\right]\left[Y_f^h\right] + \left[C_t^T\right]\left[Y_t^h\right] + \left[Y_{load}^h\right] + \left[Y_{sc}^h\right] + \left[Y_{ppf}^h\right] \tag{31}$$

For HPF studies, the slack bus is commonly considered as a stiff voltage source that is short-circuited to the ground [14]. Therefore, the admittance value of the slack bus admittance becomes very high, which is defined in this study as:

$$y_{slack}^h = 10^{10} + h \cdot j10^{10} \tag{32}$$

Then, the fundamental ($h = 1$) and harmonic branch current are computed by (33) and (34), where I_f and I_t are the *from* and *to* branch currents, respectively.

$$I_f^h = Y_f^h V_{bus}^h \tag{33}$$

$$I_t^h = Y_t^h V_{bus}^h \tag{34}$$

III. PROPOSED ALGORITHM

In this section, the modification procedures in Matpower for solving the HPF are proposed. A flowchart of the proposed algorithm for the modification procedures is presented in Fig. 5.

A. Y_{BUS} MODIFICATION FOR FUNDAMENTAL POWER FLOW

The first procedure is used to modify the formation algorithm of the fundamental $Y_{bus}^{h=1}$ matrix by adding all the network components installed in the power systems. The pseudo-code for Algorithm 1 is shown in Fig. 6.

B. HARMONIC Y_{BUS}

In this process, two algorithms were used to build a harmonic Y_{bus}^h matrix. The first algorithm defines all the network components in the harmonic Y_{bus}^h matrix, whereas the second algorithm is used to incorporate all the network components into an $nb \times nbY_{bus}^h$ matrix for each harmonic order or a$(nb \times nb) \times nh$ harmonic $Y_{bus,nh}^h$ matrix for all harmonic orders. Both Algorithms 2 and 3 are involved in the makeYbus_harmonic M-file. The pseudo-codes for Algorithms 2 and 3 are shown in Fig. 7 and 8, respectively.

C. HARMONIC POWER FLOW

In this section, the harmonic bus voltage and branch current are evaluated for every harmonic order in Fig. 9 and 10, respectively. The proposed algorithm in harmonicpf M-file calls the output from Algorithms 2 and 3, while the harmonic evaluation of voltage and current are performed in Algorithm 4 and Algorithm 5, respectively.

The harmonic bus voltages for each harmonic order are evaluated as follows:

$$V_{bus}^h = \left[Y_{bus}^h\right]^{-1} I_{inj}^h \tag{35}$$

In addition, the total harmonic distortion of voltage (TVHD) and current (TCHD) are expressed by (36) and

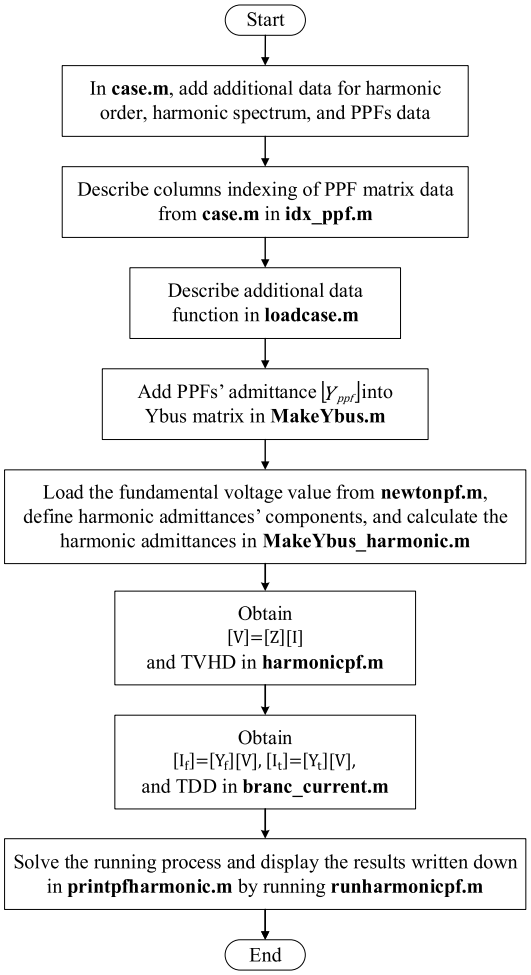

FIGURE 5. Flowchart of the modification procedures in Matpower.

Algorithm 1 PPFs modeling in fundamental $Y_{bus}^{h=1}$ matrix

Input: case M-file

Output: fundamental $Y_{bus}^{h=1}$

```
Original Y_bus^{h=1} algorithm from original MATPOWER
...
Calculate the impedance of PPF, X_{C,i} and X_{L,i}
switch ppf type
    case 1 ← single-tuned ppf
        Z_PPF^{h=1} ← Eqn. (14)
    case 2 ← second-order damped ppf
        Z_PPF^{h=1} ← Eqn. (15)
    case 3 ← third-order damped ppf
        Z_PPF^{h=1} ← Eqn. (16)
    case 4 ← C-type ppf
        Z_PPF^{h=1} ← Eqn. (17)
end switch
Y_PPF^{h=1} ← 1 / Z_PPF^{h=1}
Y_bus^{h=1} ← Eqn. (28) ▷ with installed PPF
```

FIGURE 6. Pseudo-code for Algorithm 1.

(37), respectively, and the total demand distortion (TDD) is expressed by (38), where $I_{L,ij}^{h=1}$ is the maximum demand load current of the fundamental frequency element at the point of common coupling (PCC) branch-ij.

$$TVHD_i = \frac{\sqrt{\sum_{h=2}^{n}\left(V_i^h\right)^2}}{V_i^{h=1}} \tag{36}$$

$$TCHD_{ij} = \frac{\sqrt{\sum_{h=2}^{n}\left(I_{ij}^h\right)^2}}{I_{ij}^{h=1}} \tag{37}$$

$$TDD_{ij} = \frac{\sqrt{\sum_{h=2}^{n}\left(I_{ij}^h\right)^2}}{I_{L,ij}^{h=1}} \tag{38}$$

For a steady-state analysis, where the power system is operated under the full-load condition, TCHD is equal to the TDD. In the modified Matpower, a steady-state analysis

$$C_f = \begin{cases} 1, & \text{if the } i\text{-th branch is incident to and oriented away from the } j\text{-th bus} \\ 0, & \text{if the } i\text{-th branch is not incident to} j\text{-th bus} \end{cases} \tag{22}$$

$$C_t = \begin{cases} 1, & \text{if the } i\text{-th branch is incident to and oriented toward the } j\text{-th bus} \\ 0, & \text{if the } i\text{-th branch is not incident to } j\text{-th bus} \end{cases} \tag{23}$$

$$\boldsymbol{C_f} = \begin{array}{c} \\ 1 \\ 2 \\ 3 \\ 4 \\ 5 \end{array} \begin{array}{c} \begin{array}{cccccc} ① & ② & ③ & ④ & ⑤ & ⑥ \end{array} \\ \begin{bmatrix} \mathbf{1} & \mathbf{0} & \mathbf{0} & \mathbf{0} & \mathbf{0} & \mathbf{0} \\ \mathbf{0} & \mathbf{1} & \mathbf{0} & \mathbf{0} & \mathbf{0} & \mathbf{0} \\ \mathbf{0} & \mathbf{1} & \mathbf{0} & \mathbf{0} & \mathbf{0} & \mathbf{0} \\ \mathbf{0} & \mathbf{0} & \mathbf{0} & \mathbf{1} & \mathbf{0} & \mathbf{0} \\ \mathbf{0} & \mathbf{0} & \mathbf{0} & \mathbf{0} & \mathbf{1} & \mathbf{0} \end{bmatrix} \end{array} \tag{24}$$

$$\boldsymbol{C_t} = \begin{array}{c} \\ 1 \\ 2 \\ 3 \\ 4 \\ 5 \end{array} \begin{array}{c} \begin{array}{cccccc} ① & ② & ③ & ④ & ⑤ & ⑥ \end{array} \\ \begin{bmatrix} \mathbf{0} & \mathbf{1} & \mathbf{0} & \mathbf{0} & \mathbf{0} & \mathbf{0} \\ \mathbf{0} & \mathbf{0} & \mathbf{1} & \mathbf{0} & \mathbf{0} & \mathbf{0} \\ \mathbf{0} & \mathbf{0} & \mathbf{0} & \mathbf{1} & \mathbf{0} & \mathbf{0} \\ \mathbf{0} & \mathbf{0} & \mathbf{0} & \mathbf{0} & \mathbf{1} & \mathbf{0} \\ \mathbf{0} & \mathbf{0} & \mathbf{0} & \mathbf{0} & \mathbf{0} & \mathbf{1} \end{bmatrix} \end{array} \tag{25}$$

Algorithm 2 Network components definition in harmonic Y_{bus}^h

Input: case M-file and fundamental voltage (V) from `newtonpf` in the original MATPOWER

Output: Y_{bus}^h and $I_{inj,i}^h$

Initialization:

Extract case data
Initialize parameters, `nb` and `nh`
Call indexing M-files
Grab fundamental voltage data, V

Define network components from Section 4 in Y_{bus}^h matrix:

Linear and nonlinear loads:

for $i = 1, 2, \ldots, nb$, **do**
  if $P_{d,i} = 0$ **and** $Q_{d,i} = 0$ **then**
    $r_{d,i}, x_{d,i} \leftarrow 0$
  else $r_{d,i}, jx_{d,i} \leftarrow$ Eqn. (6)
  end if
end for

Nonlinear loads:

$nlbus = [\, bus_i]$ ▷ defines the nonlinear load sitting
Calculate harmonic current injection, $I_{inj,i}^h \leftarrow$ Eqn. $(8-10)$

Shunt capacitors:

Grab shunt capacitor data from bus matrix
for $i = \text{find}(B_{sh})$, **do**
  $x_{sc,i} \leftarrow$ Eqn. (12)
end for

Passive power filters:

Grab R, X_L, and X_c from PPF matrix

FIGURE 7. Pseudo-code for Algorithm 2.

Algorithm 3 Network components modeling of harmonic Y_{bus}^h

This algorithm is the continuation of Algorithm 2.

for h and $h \neq 1$ **do**
  $Y_{br,ij}^h \leftarrow$ Eqn. $(4-5)$ ▷ series admittance
  $Y_{load,i}^h \leftarrow$ Eqn. (7) ▷ load admittance
  for $i = \text{find}(B_{sh,i})$, **do** ▷ defines the capacitor sitting
    $Y_{sc,i}^h \leftarrow$ Eqn. (13) ▷ shunt capacitor admittance
  end for
  Build C_f and C_t connection matrices
  Build network admittance matrices $\leftarrow$ Eqn. $(22-23)$
  Calculate the impedance of PPF
  switch ppf_{type}
    case 1
      $Z_{PPF}^h \leftarrow$ Eqn. (14)
    case 2
      $Z_{PPF}^h \leftarrow$ Eqn. (15)
    case 3
      $Z_{PPF}^h \leftarrow$ Eqn. (16)
    case 4
      $Z_{PPF}^h \leftarrow$ Eqn. (17)
  end switch
  $Y_{PPF}^h \leftarrow \dfrac{1}{Z_{PPF}^h}$
  $Y_{bus}^h \leftarrow$ Eqn. (31) ▷ with installed PPF
  Change $y_{slack}^h \leftarrow$ Eqn. (32)
end for

FIGURE 8. Pseudo-code for Algorithm 3.

is used. Therefore, instead of calculating the TCHD, the TDD was used to analyze the impact of harmonic distortion on power systems. Subsequently, to simplify the executing process, Algorithm 6 is used to efficiently simulate the FPF and HPF.

D. MODIFIED CASE SOLVER

In the original Matpower, an FPF is executed by running the runpf M-file. However, because there are some additional

Algorithm 4 Harmonic voltages evaluation

Input: case M-file, fundamental voltage (V) from `newtonpf` in the original MATPOWER, and results of previous algorithm

Output: V_i^h and $THD_{V,i}$

Extract case data
Initialize parameters, `nb`, `nl`, and `nh`
Grab Y_{bus}^h and I_{inj}^h from Algorithm 2 and 3
for h and $h \neq 1$ **do**
  $V_{bus}^h \leftarrow$ Eqn. (35)
end for
Calculate $TVHD_i \leftarrow$ Eqn. (36)

FIGURE 9. Pseudo-code for Algorithm 4.

Algorithm 5 Harmonic voltages evaluation

Input: case M-file, fundamental voltage (V) from `newtonpf` in the original MATPOWER, and results of previous algorithm

Output: I_f^h, I_t^h, and TDD_{ij}

Extract case data
Initialize parameters, `nb`, `nl`, and `nh`
Grab V_{bus}^h from Algorithm 4, Y_f^h, and Y_t^h
for h **do**
  $I_f^h \leftarrow$ Eqn. (33)
  $I_t^h \leftarrow$ Eqn. (34)
end for
Calculate $TDD_{ij} \leftarrow$ Eqn. (38)

FIGURE 10. Pseudo-code for Algorithm 5.

Algorithm 6 Harmonic power flow solver

Input: `casedata`, `mpopt`, `fname`, `solvedcase`

Initialization:

Extract case data
Initialize paremeters, `nb`, `nl`, and `nh`
Copy `runpf` algorithm into `runharmonicpf` algorithm
Change casedata to the modified case M-file, casedata = 'case'
Call indexing M-files
…
Modify internal index in `runharmonicpf` and add `nlbus`, `ppf`, `h`, `Ih`
…
Call output from `makeYbus_harmonic`, `harmonicpf`, and `branch_current`
…
Modify '`output result`' in `runpf` and add `nlbus`, `ppf`, `h`, `Ih`
…
Call `printharmonicpf` M-file to display the output result of the running process on the command windows

FIGURE 11. Pseudo-code for Algorithm 6.

data in the proposed modified Matpower, modifying the runpf M-file is mandatory. This modification is made in the runharmonicpf M-file.

The input data in this function are the modified case and the initial mpopt, fname, and solvedcase from the original Matpower. A new script for the case solver is shown in Fig. 11.

E. MODIFIED PRINTHARMONICPF

The last modification is to customize the output function, called printharmonicpf. To avoid repeated printing, the runharmonicpf calls the modified printharmonicpf instead of printpf. Any results can be displayed after extracting the printharmonicpf in this M-file. In this study, the printpfharmonic was modified to display the FPF, and for the HPF

TABLE 2. Taipower 38 Bus distribution loads.

Bus	Linear Loads		Nonlinear Loads	
	P (kW)	Q (kVAR)	P (kW)	Q (kVAR)
2	8000.00	0.00	0	0
4	22.50	13.95	22.50	13.95
9	67.50	41.85	37.50	23.25
10	15.00	9.30	0	0
11	15.00	9.30	0	0
13	90.00	55.80	45.00	27.90
14	90.00	55.80	0	0
15	9.00	5.580	0	0
16	22.50	13.95	22.50	13.95
18	90.00	55.80	180.00	111.60
19	90.00	55.80	45.00	27.90
21	15.00	9.30	0	0
22	67.50	41.85	52.50	32.55
23	15.00	9.30	0	0
24	15.00	9.30	0	0
25	45.00	27.9	0	0
26	15.00	9.30	0	0
27	105.00	65.10	300.00	186.00
29	105.00	65.10	90.00	55.80
30	60.00	37.20	0	0
33	67.50	41.85	37.50	23.25
34	30.00	18.60	0	0
35	15.00	9.30	0	0
36	45.00	27.90	193.50	119.97
37	45.00	27.90	0	0
38	15.00	9.30	0	0

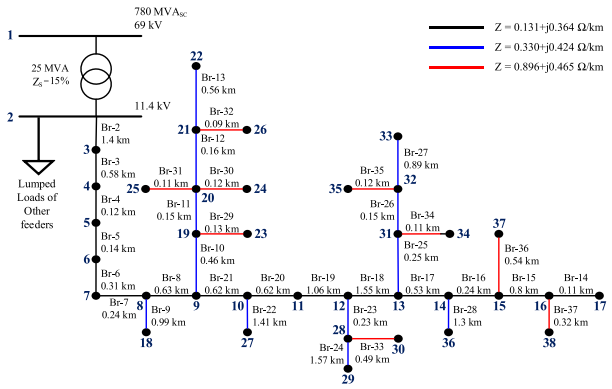

FIGURE 12. Taipower 38 Bus distribution system.

study, it displays the TVHD at all buses and TDD at all branches.

IV. RESULT AND DISCUSSION

In this section, a practical Taipower-38 bus distribution system [15] is analyzed. The one-line diagram of the test feeder is presented in Fig. 12, and the modified parameters in the distribution loads are listed in Table 2.

Three case studies were conducted in the simulation analysis. Initially, for case study 1, a base case was used without installing SCs or PPFs. Then, the bus voltages and branch currents for the FPF and HPF were calculated. To assure the accuracy of the modified Matpower, the Open Distribution System Simulator (OpenDSS) [16] was used as a benchmark

TABLE 3. Simulation results of case study 1 at PCC.

Parameter	Value
Fundamental voltage at the PCC (per unit)	0.955643
TVHD at the PCC (%)	3.83
TDD of the branch current (%)	17.76

TABLE 4. Installed shunt capacitor parameters.

Bus	Fundamental Volt. (pu)	Shunt Capacitors		Fundamental Volt. (pu) with SCs
		kVAR	Quantity	
14	0.957123	5	2	0.958357
16	0.956907	5	1	0.958172
36	0.955643	5	4	0.956959
37	0.956813	5	1	0.958066
38	0.956861	5	1	0.958132

for comparison, and the percentage errors between the simulation results were evaluated using (39). For case study 2, SCs were installed in the power system, injecting reactive power and reducing reactive PF. The system bus voltage was fixed with the appropriate sizing and siting of the SCs. However, harmonic resonance occurred and multiplied the harmonic distortion in the power system. Hence, in case study 3, the PPFs were installed to adequately reduce the harmonic distortion. The simulation results are presented and discussed below.

$$\%Errors = \left| \frac{f_i^{matpower} - f_i^{opendss}}{f_i^{opendss}} \right| \times 100 \qquad (39)$$

A. CASE STUDY 1

Initially, a base case system of Taipower 38 bus was simulated for the FPF and HPF analyses. In terms of accuracy, the maximum fundamental voltage and angle errors were 0.000488% and 0.000113%, respectively. Moreover, for the HPF analysis, the maximum harmonic voltage error was 0.004568%. The minor errors confirm the accuracy of the modified Matpower.

In this case study, the PCCs for the HPF analysis were set at every nonlinear load bus. As nonlinear loads injected harmonic currents into the power system, harmonic distortion occurred at every harmonic order. The maximum TVHD appeared at bus 36, later referred to as PCC, with a value of 3.83%, which is within the limitation set by IEEE Std. 519. However, the TDD and some individual current harmonic distortions (ICHD) at the PCC branch exceeded the IEEE Std. 519 limit, as presented in Table 3. The radar charts of the current and voltage harmonic distortion for the individual harmonic order (IHD) are presented in Fig. 13 (a) and (b), respectively.

From the figures, even when the bus voltage harmonic distortion is within the limit, the branch current harmonic distortion may exceed the restriction. Therefore, both the bus

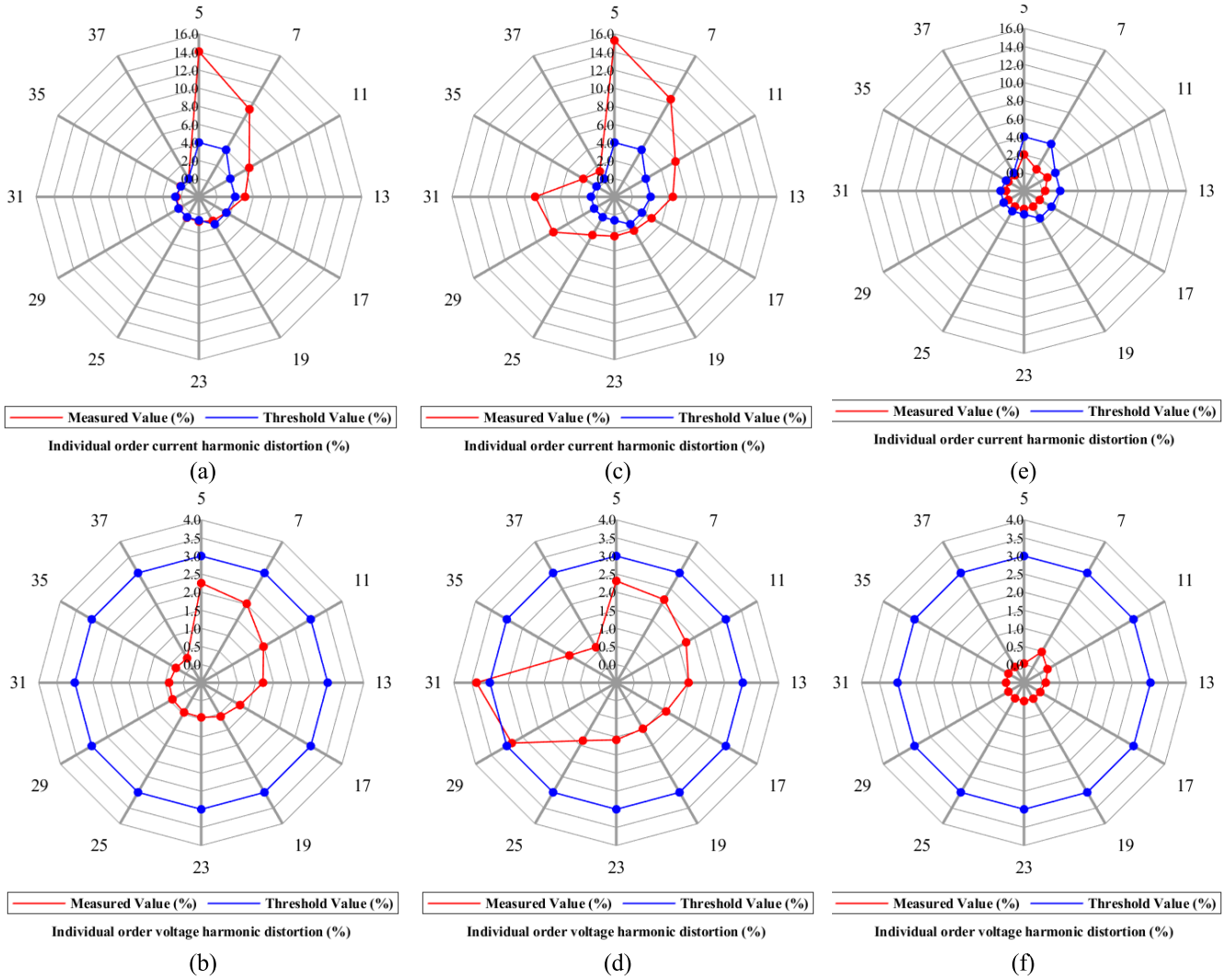

FIGURE 13. Radar charts of (a) ICHD and (b) IVHD of Case Study 1, (c) ICHD and (d) IVHD of Case Study 2, (e) ICHD and (f) IVHD of Case Study 3.

voltage and branch current harmonic distortions should be analyzed for an appropriate HPF analysis.

B. CASE STUDY 2

As described in Table 3, the fundamental voltage at the PCC was 0.956959 per unit. Although this value is under the minimal voltage limit, it can be improved by installing SCs into the power system, which compensates for the reactive power and updates the system voltages. Hence, some SCs described in Table 4 were installed at buses with lower voltages.

The simulation results described in Table 5 show the ability of the installed SCs to improve the fundamental voltage at the PCC with a lower voltage deviation. However, installing SCs may distort the branch current and bus voltage at every harmonic order. According to Fig. 13 (c) and (d), the ICHD at every harmonic order is not in accordance with the limit set by IEEE Std. 519 as the threshold values, whereas only the individual voltage harmonic distortion (IVHD) at harmonic order 31 is not in accordance. Furthermore, the maximum TVHD was 6.41% at bus 36, exceeding the 5% limit, and the maximum TDD was 22.54% at branch 28, exceeding the 5% threshold at the PCC.

TABLE 5. Simulation results of case study 2 at PCC.

Parameter	Value
Fundamental voltage at the PCC (per unit)	0.956959
TVHD at the PCC (%)	6.41
TDD of the branch current (%)	22.54

From these results, a reduction in the harmonic distortion in the power system is essential. Thus, the case study with harmonic filter compensation is analyzed in the next section.

C. CASE STUDY 3

In this case study, harmonic filter compensation was analyzed. To reduce the harmonic distortion of the current and voltage, some PPFs were installed in the power system,

TABLE 6. Results of the case study 3: analysis and parameters of the installed PPFs.

Specification	Threshold	Case Study 1	Case Study 2	Case Study 3		
	-	-	-	Type 2	Type 3	Type 4
	-	-	-	Bus 16	Bus 36	Bus 27
Filter parameters	-	-	-	$R = 9.17\ \Omega$	$R = 0.182\ \Omega$	$R = 1349\ \Omega$
	-	-	-	$X_L = 25.8277\ \Omega$	$X_L = 0.8256\ \Omega$	$X_L = 1264.8\ \Omega$
	-	-	-	$X_C = 3.2523\ \Omega$	$X_C = 40.6218\ \Omega$	$X_C = 10\ \Omega$
Fundamental volt. at the PCC (pu)	0.9~1.1	0.955643	0.956959		1.041592	
TVHD at the PCC (%)	5	3.83	6.41		0.55	
TDD at the PCC branch (%)	5	17.76	22.54		2.40	

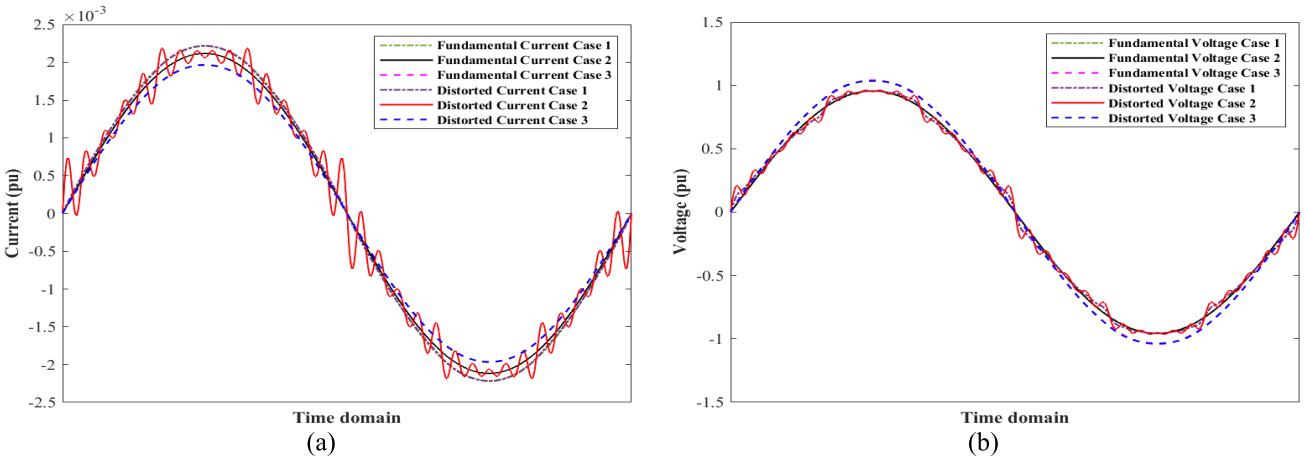

FIGURE 14. Fundamental and distorted (a) current and (b) voltage of all case studies.

as described in Table 6. The proposed modified algorithm was useful for analyzing the four types of PPF installations in the same simulation process. Different types of PFFs were used to mitigate harmonic distortions in the appropriate order. Table 6 presents the results of this case study simulation. From the results, the maximum TVHD at the PCC was reduced from 6.41% to 0.55%, which is a better result than that of case study 1. Moreover, the maximum TDD at the PCC branch showed an excellent reduction from 22.54% to 2.40%, which is below the 5% threshold. In terms of harmonic order, Fig. 13 (e) and (f) show the improvement in ICHD and IVHD at the PCC, respectively.

This analysis shows the superiority of the modified Matpower in analyzing the harmonic distortion reduction based on the different types of PPF installation in terms of various harmonic orders.

Furthermore, Fig. 14 shows the (a) current and (b) voltage waveforms for all case studies. As observed, for case study 1, the nonlinear loads injected harmonic current into the power system and distorted the current at the PCC branch and the voltage at the PCC. In the shape of the waveform, the distortion seems harmless. However, in terms of IHD, the values were significant. A small contribution of the elements had a massive impact on the power system. This was clarified by case study 2, where some SCs were installed in the system. From Table 4, the installed SCs contributed to a minor kvar. Nonetheless, SCs supplied an extensive distortion of the branch current and bus voltage. Fig. 14 shows that the distorted current ripples multiplied the TDD at the PCC branch more than half of the time, and the TVHD at the PCC was almost double the value than before Consequently, PPFs were installed in the power system to mitigate these distortions. As shown in Fig. 14, the ripples in (a) current and (b) voltage were drastically reduced, and the waveform became almost perfect.

V. CONCLUSION

In this study, modification procedures were proposed to evaluate the HPF in Matpower. Previously, Matpower was used to solve FPF problems. Matpower has an adjustable feature that supports modifications to solve specific problems in power systems. The proposed modification procedures are simple and adjustable to the user demand. Nonlinear loads, harmonic spectra, and PPF parameters are added in HPF study. Moreover, admittance modeling was modified to support HPF study analysis.

Some accuracy tests were performed and indicated the ability of the modified Matpower to evaluate the HPF study. The differences between the simulation results obtained by the modified Matpower and OpenDSS can be neglected. Furthermore, the modification achieves a better analysis with a simple procedure of PPF compensation than benchmark software. The installed PPFs reduced the harmonic current

and voltage, and the modified Matpower was superior in this compensation method.

REFERENCES

[1] R. C. Dugaan, M. F. McGranaghan, and S. Santosa, *Electrical Power Systems Quality*. New York, NY, USA: McGraw-Hill, 2003.

[2] J. Grainger and S. Lee, "Optimum size and location of shunt capacitors for reduction of losses on distribution feeders," *IEEE Trans. Power App. Syst.*, vol. PAS-100, no. 3, pp. 1105–1118, Mar. 1981.

[3] Y. Baghzouz, "Effects of nonlinear loads on optimal capacitor placement in radial feeders," *IEEE Trans. Power Del.*, vol. 6, no. 1, pp. 245–251, Jan. 1991.

[4] N. E. Chang, "Locating shunt capacitors on primary feeder for voltage control and loss reduction," *IEEE Trans. Power App. Syst.*, vol. PAS-88, pp. 1574–1577, Oct. 1969.

[5] E. F. Fuchs and M. A. S. Masoum, *Power Quality in Power Systems and Electrical Machines*. New York, NY, USA: Academic, 2008.

[6] *IEEE Guide for the Application of Shunt Power Capacitors*, IEEE Standard 1036-2020 (Revision of IEEE Std 1036-2010), 2021, pp. 1–96.

[7] S. H. Hamouda, S. H. E. A. Aleem, and A. M. Ibrahim, "Harmonic resonance index and resonance severity estimation for shunt capacitor applications in industrial power systems," in *Proc. 19th Int. Middle East Power Syst. Conf. (MEPCON)*, Dec. 2017, pp. 527–532.

[8] N.-C. Yang and M.-D. Le, "Optimal design of passive power filters based on multi-objective bat algorithm and Pareto front," *Appl. Soft Comput.*, vol. 35, pp. 257–266, Oct. 2015.

[9] B. Alamri, C. Marouchos, and M. Darwish, "Optimum design of passive power filter (PPF) at the output of 5-level CHB-MLI using genetic algorithm (GA)," in *Proc. 52nd Int. Univ. Power Eng. Conf. (UPEC)*, Aug. 2017, pp. 1–6.

[10] Y.-P. Chang and C.-N. Ko, "A PSO method with nonlinear time-varying evolution based on neural network for design of optimal harmonic filters," *Expert Syst. Appl.*, vol. 36, no. 3, pp. 6809–6816, Apr. 2009.

[11] R. D. Zimmerman, C. E. Murillo-Sánchez, and R. J. Thomas, "MATPOWER: Steady-state operations, planning and analysis tools for power systems research and education," *IEEE Trans. Power Syst.*, vol. 26, no. 1, pp. 12–19, Feb. 2011.

[12] R. D. Zimmerman, C. E. Murillo-Sánchez, D. Gan, and R. J. Thomas, "Matpower," 7.1st ed., Tech. Rep., 2020.

[13] S. H. H. Sadeghi, S. M. Kouhsari, and A. Der Minassians, "The effects of transformers phase-shifts on harmonic penetration calculation in a steel mill plant," in *Proc. 9th Int. Conf. Harmon. Quality Power.*, vol. 3, 2000, pp. 868–873.

[14] N. Yang and M. Le, "Three-phase harmonic power flow by direct Z_{BUS} method for unbalanced radial distribution systems with passive power filters," *IET Gener., Transmiss. Distrib.*, vol. 10, no. 13, pp. 3211–3219, Oct. 2016.

[15] N.-C. Yang and T.-H. Chen, "Dual genetic algorithm-based approach to fast screening process for distributed-generation interconnections," *IEEE Trans. Power Del.*, vol. 26, no. 2, pp. 850–858, Apr. 2011.

[16] D. Montenegro and R. C. Dugan, "OpenDSS and OpenDSS-PM open source libraries for NI LabVIEW," in *Proc. IEEE Workshop Power Electron. Power Quality Appl. (PEPQA)*, May 2017, pp. 1–5.

NIEN-CHE YANG (Member, IEEE) was born in Keelung, Taiwan, in 1977. He received the B.S., M.S., and Ph.D. degrees in electrical engineering from the National Taiwan University of Science and Technology, Taipei, Taiwan, in 2002, 2004, and 2010, respectively. Since 2018, he has been a Faculty Member with the National Taiwan University of Science and Technology, where he is currently an Associate Professor of electrical engineering. His research interests include micro-grid state estimation, harmonic three-phase power flow analysis, probabilistic three-phase power flow analysis, energy loss computation in low-voltage networks, micro-grids, smart grids, and electric vehicles. He is a member of the Phi Tau Phi Scholastic Honor Society.

EUNIKE WIDYA ADINDA received the B.S. degree from Institut Teknologi Sepuluh Nopember, Indonesia, in 2019. She is currently pursuing the M.S. degree with the Electrical Engineering Department, National Taiwan University of Science and Technology, Taipei, Taiwan. Her research interests include harmonic power flow analysis, passive power filter, and radial-distribution networks.